PERGAMON

International Journal of Solids and Structures 36 (1999) 3617–3638

INTERNATIONAL JOURNAL OF SOLIDS and STRUCTURES

A boundary element formulation for a class of non-local damage models

R. García[a], J. Flórez-López[b,*], M. Cerrolaza[c]

[a] *Doctoral Researcher, Universidad Central de Venezuela, Caracas, Venezuela*
[b] *Universidad de Los Andes, Facultad de Ingeniería, Merida 5101, Venezuela*
[c] *Instituto de Materiales y Modelos Estructurales, Facultad de Ingeniería, Universidad Central de Venezuela, PO Box 50.361, Caracas 1050-A, Venezuela*

Received 13 November 1997; in revised form 13 April 1998

Abstract

This paper proposes and discusses a boundary element formulation for a particular class of non-local damage models. The formulation as well as the boundary element computational code developed during this research have proven to be very simple and efficient, providing reliable information on the strains and stresses in damage-softening models. The numerical approach uses a finite-grid to estimate the damage values. Some illustrative numerical examples, which show the simplicity and versatility of the proposed approach, are included and discussed in detail.

Keywords: Boundary elements; Damage mechanics; Non-local models

1. Introduction

As indicated by Professor Lippman in the foreword of a book on damage mechanics (Lemaitre, 1992), failure prevention of machine parts and civil engineering structures is one of the main objectives of the engineering science. Conventional fracture mechanics allows the prediction of situations in which a pre-existent crack will propagate. This is why this theory has become one of the most important branches of continuum mechanics. However, the description of the process of transformation of microvoids and microdefects into a macrocrack is equally important. This is the goal of Continuum Damage Mechanics (CDM).

The basic idea of CDM is the introduction of a new internal variable, denoted damage, and its evolution law. This variable characterizes the density of microvoids and microcracks of the material. The pioneering work of Kachanov (Kachanov, 1958) described the first uniaxial model of the damage process in metals subjected to creep. Later, the theory was extended to the three-

* Corresponding author. Fax: 00 58 74 402 869; e-mail: iflorez@ing.ula.ve

0020–7683/99/$ - see front matter
PII: S0020–7683(98)00159–0

dimensional case, ductile damage and fatigue damage (see for instance the works of Rabotnov, 1963; Lemaitre and Chaboche, 1978; Hult, 1974; Leckie and Hayhurst, 1974; Murakami, 1983). Brittle damage models for materials such as concrete or rocks started to appear during the 1980s (Mazars, 1986; Krajcinovic and Sumarac, 1989; Suaris, 1987; Lubliner et al., 1989) and the 1990s (Liqing and Katsabanis, 1997; Sellers and Scheele, 1996). Damage Mechanics concepts have also been used for the analysis of reinforced concrete and steel frames with plastic hinges (Flórez-López, 1998).

Damage mechanics problems are, of course, solved numerically. So far, the Finite Element Method (FEM) has been used for the majority of applications (Benallal et al., 1988; Ma and Kuang, 1995; Cervera et al., 1995). A recent work of Cerrolaza and García (1997) presented the analysis of tunnel excavation using the Boundary Element Method (BEM) combined with a brittle model of damage.

The mathematical aspects are more important in damage modeling than they are in other branches of material mechanics. This is due to the fact that damage models need to describe strain-softening behavior in order to characterize microscopic degradation processes. A phenomenon called 'localization' occurs in structural analyses with strain-softening models. Mathematically, localization manifests as the possible appearance of an infinite number of solutions, i.e. the problem might be ill-posed. In FEM formulations, localization appears as an unacceptable mesh dependence of the response.

Regularization techniques are therefore essential in CDM. The goal of using these techniques is to prevent, or at least to control, localization. Some of those procedures are nonlocal damage models (Pijaudier-Cabot and Bazant, 1987); Saudiris and Mazars, 1988), gradient-dependent models (Belytschko and Lasry, 1988), the use of Cosserat media (De Borst, 1990) and progressive localization (Abeyaratne and Knowles, 1990; Billardon and Flórez-López, 1991).

This paper proposes a Boundary Element Formulation for a particular class of nonlocal damage models: the grid-damage models. This regularization procedure was proposed in a paper by Hall and Hayhurst (1991) and described also by De Vree et al. (1995). In the latter, nonlocal and grid-damage models were used in numerical analyses of structures by the FEM. The present paper combines the results described in those two references with the algorithms proposed in Cerrolaza and García (1997).

Nonlocal or grid-damage analyses by the FEM require extensive modifications of the standard codes. So far, only homemade, highly specialized programs perform these analyses. Furthermore, the existing algorithms are not very efficient and are particularly expensive in terms of computer memory requirements. On the other hand, the BEM appears to be the most natural approach for grid-damage analyses. It will be shown in this paper that the BEM results in a very simple formulation for the analysis of this kind of problems and more importantly, that any existing BE program can be modified, with a very small computational effort, to include grid-damage models. In addition, all the usual advantages of the BEM over the FEM could be listed.

In the following, an overview of CDM models is given, emphasizing the necessity to use nonlocal models. This short review is essentially intended for those readers who are interested in the BEM but that are not necessarily specialists in CDM. Then, a brief description of the BEM, devoted to readers working on CDM exclusively, is included. Those reviews are followed by the BE formulation for grid-damage models. Some two-dimensional numerical examples are presented and discussed in the final section of the paper.

2. Continuum damage mechanics

2.1. Local damage approach

Continuum Damage Mechanics is based on the introduction of an additional internal variable: the damage, which characterizes the state of deterioration of a volume element in a continuum. Let A be the area of the intersection of a plane with the volume element and let A_d be the effective area of the intersections of all microcracks or microvoids in the element with A. The damage D_n in this volume element and in the direction defined by the normal **n** to the area A can be expressed as:

$$D_n = \frac{A_d}{A} \tag{1}$$

This variable can take values between zero (intact element) and one (broken element). The hypothesis of isotropic damage consists of assuming that D_n is approximately the same whatever the normal **n** is. In such a case the state of damage can be represented by a scalar:

$$D_n \cong D \,\forall\, n \tag{2}$$

Coupling between isotropic damage and elasticity can be expressed by introducing some hypotheses (Lemaitre and Chaboche, 1978), in the following way:

$$\sigma_{ij} = (1-D)H_{ijkl}\varepsilon_{kl} \tag{3}$$

where H_{ijkl} is the conventional elastic tensor.

For brittle materials (Marigo, 1982; Brekelmans et al., 1992), damage evolution can be determined as in elastoplastic models with isotropic hardening. A 'damage function' is then introduced. This function depends on some adequate invariant of the strain tensor ε_{eq} called 'equivalent strain', and on a hardening term $K(D)$:

$$f = \varepsilon_{eq} - K(D) \tag{4}$$

Damage remains constant if the function f is negative or if it is decreasing and it evolves if f is equal to zero. The term K must fulfill some conditions so that $\dot{D}$ is always positive or zero.

$$\begin{aligned} &\dot{D} > 0 \quad \text{if} \quad f = 0 \quad \text{and} \quad \dot{f} = 0 \\ &\dot{D} = 0 \quad \text{if} \quad f < 0 \quad \text{or} \quad \dot{f} < 0 \end{aligned} \tag{5a}$$

Alternatively the damage evolution law (5a) can be written as follows (see Flórez-López et al., 1994):

$$D = K^{-1}(\mathrm{Max}\,\varepsilon_{eq}) \quad \text{for} \quad 0 \leqslant D \leqslant 1 \tag{5b}$$

where $\mathrm{Max}\,\varepsilon_{eq}$ is the maximum value that the equivalent strain has taken since the beginning of the loading (or since any instant that corresponds to $D = 0$) until the present time (i.e. the one for which the damage is being calculated). Formulations (5a) and (5b) are equivalent. The form (5b) of the evolution law presents some advantages over (5a) during the numerical implementation of the model.

It can be noticed that damage depends only on the strain history of the particular volume element under consideration. This is why this approach is called 'local'.

2.2. Localization and mesh dependence of the response

Local damage models lead to unacceptable mesh dependence of the structural response when they are used with the finite element method. In this section, this mesh dependence is illustrated with the help of a very simple uniaxial example.

Let us consider a uniaxial continuum occupying the interval [0, L] subjected to the following boundary conditions: $U(0) = 0$ and $U(L) = U^d(t)$ where $U^d(t)$ is a positive and monotonic function of time. The material of this structure obeys the damage model described in the previous section with $\varepsilon_{eq} = \varepsilon$ and $K(D) = M \cdot D$ where M is a positive constant (see Fig. 1). This solid is discretized into two finite elements, with linear displacements and constant strains, such as indicated in Fig. 2. It can be noticed that, in this particular case, the finite element solution corresponds to the exact solution. The equilibrium between the two elements can be expressed simply by stating that stresses must be constant and equal in both elements. This equilibrium condition can be represented as a

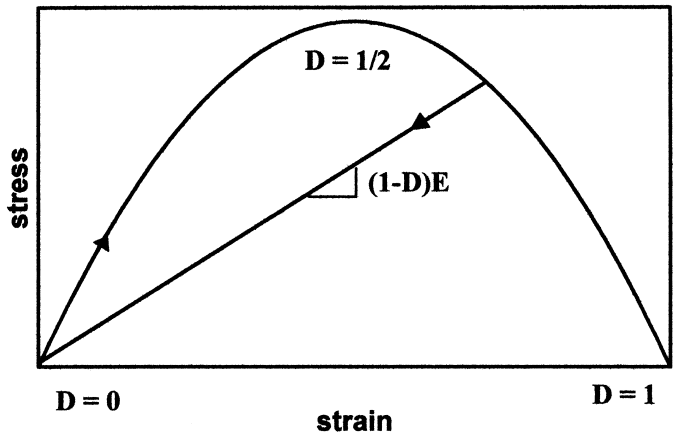

Fig. 1. Stress as a function of the strain in a brittle damage model.

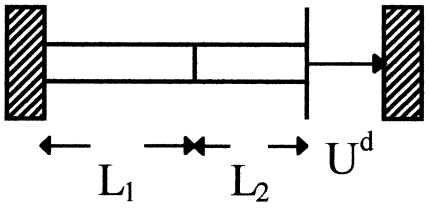

Fig. 2. Two-element model subjected to imposed displacements.

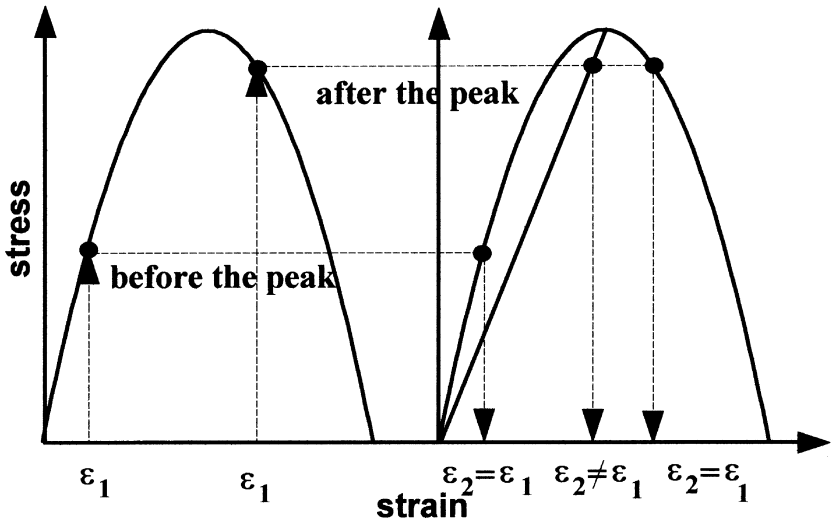

Fig. 3. Constitutive laws and equilibrium conditions for the model of Fig. 2.

horizontal line in a graph where the constitutive equations of both elements are simultaneously represented (see Fig. 3).

Let us consider an increment in the imposed displacement such that the strain in the first element (denoted as ε_1 in Fig. 3) corresponds to a point that has not yet reached the peak of the curve in Fig. 3. Then, there is only one solution that verifies the equilibrium condition and this solution imposes that the strain in the second element (denoted as ε_2 in Fig. 3) must be equal to the strain in the first element.

Let us now consider an increment of the displacement such that the strain in the first element corresponds to a point after the peak of the curve in Fig. 3. In such a case, there are two solutions that verify the equilibrium condition. The first solution corresponds to a constant state of strains and damage throughout the solid. The second solution imposes an elastic unloading in the second element and a discontinuous state of damage. This discontinuity should not be confused with those that appear in finite element analyses due to the discretization of the solid. That kind of discontinuity tends to disappear with the refinement of the mesh when the finite element solution tends to the exact solution, which is not the case here. Remember that in this very simple example, the model with two elements gives exact solutions.

The appearance of discontinuities in the strain and damage, when there are no other sources of discontinuities such as change of material, is called in the literature 'localization'. The two force-displacement curves that characterize the global response of the structure are shown in Fig. 4. It can be easily found that the failure of the solid (D equal to one in at least one element) corresponds to a displacement equal to $M \cdot L$ for the homogeneous solution and $M \cdot L_1$ for the localized solution. However, the length L_1 of the localization zone is a property of the mesh and therefore the solution is mesh-dependent. This very simple example also shows that local damage models can lead to problems that may have an infinite number of solutions since any length L_1 between zero and L could be used in the FE mesh. It is said then that the problem is 'ill posed'.

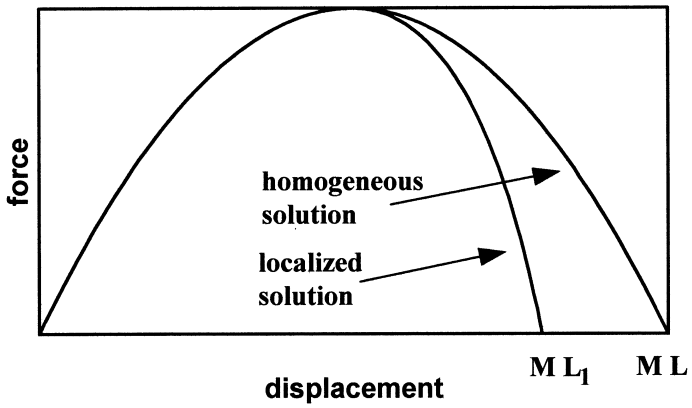

Fig. 4. Force as a function of the displacement for the model of Fig. 2.

In De Vree et al. (1995), the same kind of mesh dependence for two-dimensional problems solved by the finite element method is shown.

2.3. Nonlocal damage models

The mesh dependence shown in the example of the previous section is obviously unacceptable. Thus, some kind of regularization is needed if a damage model is to be used. In this section, one of the alternatives that have been proposed in the literature is described. Specifically, the case of nonlocal damage models is considered.

The basic hypothesis of the nonlocal damage regularization is that mesh dependence and ill-posedness of the problem are due to localization of damage and strains rather than being one of the symptoms of the mathematical ill-posedness of the problem. Therefore, the idea is to modify the constitutive law in such a way that localization (or damage discontinuities) is avoided or at least controlled. This is done by neglecting the local action principle. Damage is now assumed to depend not only on the state of the particular volume element but also on the state in a limited zone enclosing the specific point under consideration. A nonlocal damage model can be formulated as follows (Pijaudier-Cabot and Bazant, 1987; Saudiris and Mazars, 1988):

$$\begin{aligned} &\sigma_{ij} = (1-D)H_{ijkl}\varepsilon_{kl} \quad \text{(state law)} \\ &f = \bar{\varepsilon}_{\text{eq}} - K(D) \quad \text{(damage function)} \end{aligned} \tag{6}$$

where $\bar{\varepsilon}_{\text{eq}}$ represents an average of ε_{eq} in the neighborhood of the volume element. It can be noticed that only the damage evolution law is modified with respect to the local modeling. The way in which the average of equivalent strain is calculated leads to different nonlocal models. For instance, in Pijaudier-Cabot and Bazant (1987), the following expression is proposed:

$$\bar{\varepsilon}_{\text{eq}} = \frac{1}{V_r(x)} \iiint_v \alpha(s-x)\varepsilon_{\text{eq}}(x)\,\mathrm{d}v(s); \quad V_r(x) = \iiint_v \alpha(s-x)\,\mathrm{d}v(s) \tag{7}$$

where α is an empirical weighting function, x and s are the coordinate vectors and V is the volume

of the body. With this model, any concentration of strains will have a transfer to the neighborhood that will prevent damage localization. This kind of nonlocal model seems to lead to continuum damage fields (De Vree et al., 1995).

2.4. Grid damage models

Another variation of the nonlocal approach is constituted by the 'grid damage models' (Hall and Hayhurst, 1991). This can be considered as a simplification of the strategy described in section 2.3 and is inspired in the observation that many materials have a characteristic volume where damage is almost uniform. In this section the grid method will be presented as described in De Vree et al. (1995) and in section 4 of this paper a boundary element formulation for this nonlocal model will be proposed.

In grid models, a regular cell grid is placed on the solid under consideration. The measures of the cell are equal to a characteristic material parameter λ. Within each cell the damage state is assumed to be constant and depends on the average of the equivalent strains ε_{eq} in the cell. This can be expressed as

$$\begin{aligned} &\sigma_{ij} = (1-D)H_{ijkl}\varepsilon_{kl} \quad \text{(state law)} \\ &D(x) = D^k \quad \text{if} \quad x \in V^k \\ &f^k = \bar{\varepsilon}^k_{eq} - K(D^k) \end{aligned} \tag{8}$$

where V^k denotes the domain of the k-th cell of the grid, D^k is the damage of the cell, f^k is the damage function of the cell and $\bar{\varepsilon}^k_{eq}$ is the equivalent strain of the cell, calculated as:

$$\bar{\varepsilon}^k_{eq} = \frac{1}{V^k}\iiint_{v^k} \varepsilon_{eq}(x)\,\mathrm{d}v \tag{9}$$

It is important to underline that this grid is independent of the discretization used for the numerical resolution of the problem (see Fig. 5). In De Vree et al. (1995), a finite element formulation for this kind of model is presented and the convergence of the solution with the refinement of the mesh is shown for some two-dimensional examples. Comparisons between local and grid damage models are also shown in that paper. Nonlocal grid models are very simple and can be an effective engineering tool for the evaluation of the safety of structures.

3. The boundary element method

The boundary element method is a well-known numerical procedure for the resolution of integral equations with boundary conditions. A brief summary of the method will be included herein for consistency. The reader interested in the details of the formulation is referred to Brebbia et al. (1984); Crouch and Startfield (1983) and Kane (1994), among other related books on the subject.

For linear elastic problems, the method is based on the Betti's reciprocal theorem that is applied in the following way:

Let V be a body with boundary S, the part of S where the displacements U_i^{d} are known is denoted S_u, and the part where known tractions T_i^{d} are applied, is represented by S_t. The problem,

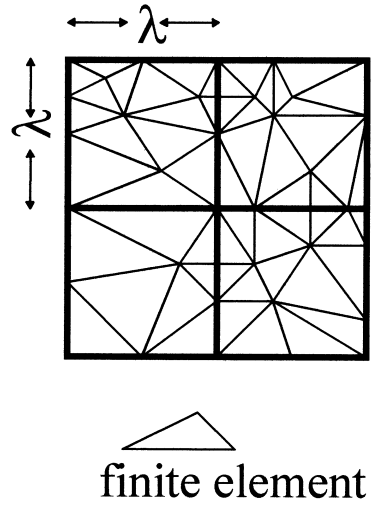

Fig. 5. Finite element mesh and cell grid.

called 'real', consists in the calculation of the displacement, stress and strain fields due to these external actions. The resolution of the real problem requires the statement of an auxiliary problem, called 'fictitious'. In this problem a body with the same geometry (defined by V and S) of the real problem is subjected to a unit concentrated load on a source point P of the solid in the direction of an axis x_i. The application of the reciprocal theorem for the real and fictitious problem leads to:

$$u_i(P) = \iint_S [U_{ij}(P,Q)t_j(Q) - T_{ij}(P,Q)u_j(Q)]\,\mathrm{d}S \tag{10}$$

where $u_i(P)$ represents the displacement of a point P in the direction of x_i, the capital U_{ij} and T_{ij} are the displacements and tractions on a point Q of the surface of the body, in the fictitious problem, and in the direction x_j. These terms have been calculated analytically for an infinite medium and are called 'Kelvin solutions':

$$U_{ij}(P,Q) = \frac{1}{8\pi G(1-\upsilon)}\left[(3-4\upsilon)\log\left(\frac{1}{r}\right)\delta_{ij} + r_{,i}r_{,j}\right]$$

$$T_{ij}(P,Q) = -\frac{1}{4\pi(1-\upsilon)}\frac{1}{r}\{[(1-2\upsilon)\delta_{ij} + 2r_{,i}r_{,j}]r_{,n} - (1-2\upsilon)(r_{,i}n_j - r_{,j}n_i) \tag{11}$$

where ν and G are coefficients of the isotropic elastic law and r is the distance between the points P and Q.

Equation (10) allows the computation of the displacements, and therefore of the strains and stresses, of the real problem in any point of the body as a function of the values of the displacements and tractions on the boundary of the solid. However, for the real problem, displacements and tractions are not known simultaneously in any point of the surface S. For the calculation of the unknown terms, eqn (10) is also applied to the points of the body's surface. Nonetheless, if P is

on the boundary, a singularity occurs in the integration as the point Q is approached (i.e. the term $T_{ij}(P, Q)$ becomes infinite). Therefore numerical integration of (10) must be done by using special quadrature formulas (Gray, 1993; Chen et al., 1990; Cerrolaza and Alarcón, 1989).

For the numerical determination of the unknown in the boundary, this surface is discretized in elements that are essentially the same as finite elements except that their dimension is reduced by one. These elements can be described as follows:

$$t_i = N_j b_i^j, \quad u_i = N_j a_i^j \tag{12}$$

where N_j are the interpolation functions, a_i^j are the nodal displacements on the boundary and b_i^j the nodal tractions.

The application of the discretized version of (10) to each node of the body's surface leads to a linear matrix equation of the form:

$$[A]\{a\} = [B]\{b\} \tag{13}$$

where $[A]$ and $[B]$ are coefficient matrices. In the present context it is important to underline that these matrices depend on the elastic properties of the material through the constants G and v in (11). Equation (13) plus the boundary conditions of the real problem, allow for the computation of the unknown terms of $\{a\}$ and $\{b\}$.

After the computation of the nodal unknowns, displacements, strains or stresses can be calculated at any point of the body.

4. Boundary element formulation for grid damage models

4.1. Formulation

Let us consider an isotropic elastic damageable body that obeys the constitutive law described in section 2.4. For each cell in the structure, two problems are again under consideration:

(a) The real one that consists of a cell under the boundary conditions imposed by the surrounding cells and, if the cell in question is on the surface of the structure, the external actions.
(b) The fictitious one that involves the same cell of an elastic damageable material with a constant state of damage equal to D^k and subjected to a unitary force such as described in section 3.

Application of eqn (10) for each cell k of the grid leads to:

$$u_i(P) = \iint_{V^k} [U_{ij}(P,Q;D^k)t_j(Q) - T_{ij}(P,Q;D^k)u_j(Q)]\,\mathrm{d}S \quad P \in V^k \quad Q \in S^k \tag{14}$$

where V^k represents again the k-cell of the grid and S^k its boundary.

In the conventional boundary element method, displacements or tractions are known on the boundary under consideration. This is not the case for the cells where neither displacements nor tractions are known, if a surface of the cell does not coincide with the border of the body. However, the boundary conditions can be substituted by the compatibility and equilibrium equations that state the continuity of displacements and tractions across the boundary S_l^k between two adjacent cells k and l:

$$u_i^+(Q) = u_i^-(Q) \quad t_i^+(Q) = t_i^-(Q) \quad \forall Q \in V^k \bigcap V^l = S_l^k \tag{15}$$

where the symbols + or − indicates a quantity in the cell k or l, respectively.

It must be underlined that eqn (14) depends on the damage of the cell because this variable modifies the elastic properties of the material, i.e. the elastic constant G in (11) must be substituted by $(1-D^k)G$ when used for a damaged cell k.

Therefore, eqn (14), the boundary conditions, the compatibility and equilibrium eqns (15) and the damage evolution law of each cell (16) define a boundary element formulation for a grid-damage model.

$$\begin{aligned} &f^k = \bar{\varepsilon}_{\text{eq}}^k - K(D^k) \\ &\begin{cases} \dot{D}^k = 0 & \text{if} \quad f^k < 0 \quad \text{or} \quad \dot{f}^k < 0 \\ \dot{D}^k > 0 & \text{if} \quad f^k = 0 \quad \text{and} \quad \dot{f}^k = 0 \end{cases} \end{aligned} \tag{16}$$

4.2. Numerical implementation

A conventional step-by-step procedure is adopted for the numerical resolution of the problem. Then, the damage evolution law (5a) is discretized as follows:

$$\begin{cases} f^k(\varepsilon, D^k) = 0 & \text{if damage is active in cell } k \\ \Delta D^k = 0 & \text{otherwise} \end{cases} \tag{17}$$

where ΔD^k represents the increment of damage during the step. Here, the terms ε and D^k are the values of these variables at the end of the step. If the form (5b) of the damage evolution law is used, then discretization consists, simply, in the calculation of Max $\bar{\varepsilon}_{\text{eq}}$ taking into account the equivalent strain only at the end of the steps instead of considering the entire strain history.

Every cell is discretized using the boundary elements (see Fig. 6). Therefore, we have for each step and for each cell

$$[A^k(D^k)]\{a^k\} = [B^k(D^k)]\{b^k\} \tag{18}$$

The compatibility and equilibrium eqns (15) can be taken into account by an adequate assemblage of matrices $[A^k]$ and $[B^k]$ of each cell into the global matrices $[A]$ and $[B]$ resulting in a system of equations of the conventional form:

$$[A(D)]\{a\} = [B(D)]\{b\} \tag{19}$$

The nonlinear system of equations composed by (17, 19) can be solved by a conventional direct iteration algorithm in which the computation of the state of the body $(U(x); D(x))$ at a time t_i is obtained by the following procedure:

(a) The field $D(x) = D^0$ (damage field at the iteration zero) is taken as the damage field at time t_{i-1}.
(b) The displacement field $\mathbf{U}(x) = \mathbf{U}^j$ (displacement field at the iteration j) is computed by the resolution of (18) using the damage field at the iteration $j-1$.

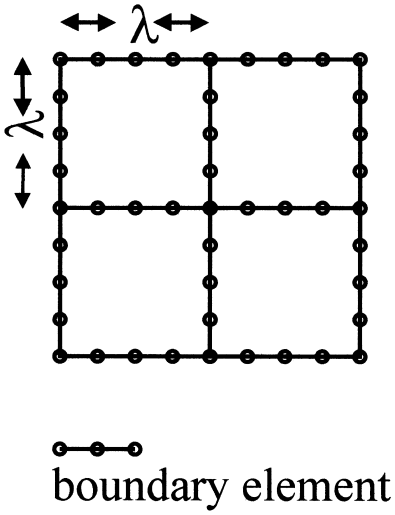

Fig. 6. Boundary element mesh.

(c) The damage field $D(x) = D^j$ (damage field at the iteration j) is calculated by the resolution of (17) using the displacement field at the iteration j.
(d) Convergence of the algorithm is checked. If there is no convergence, a new iteration is needed starting by step (b).

If the form (5b) of the damage evolution law is chosen, then step (c) is straightforward, the maximum equivalent strain is calculated taking into account only the set of values at the end of each step. Otherwise, i.e. if expression (5a) is used, a predictor-corrector algorithm should be used. This consists in the evaluation of the damage function $f(D^k, \bar{\varepsilon}_{eq})$ with the damage at the beginning of the step and the equivalent strain at the end of the step. If this function is negative or zero then damage remains constant during the step, otherwise the damage at the end of the step is computed making the damage function equal to zero.

5. Numerical examples

5.1. Definition of the damage function

This section presents and discusses two numerical examples analyzed with the approach proposed in this work.

A computer program, based on the formulation and the algorithm described in section 4, was developed. The model proposed by Mazars (1986) was adapted to the grid scheme presented in section 2.4 and included in the program. This was done by using the following expressions:

$$\varepsilon_{eq} = \sqrt{\langle \varepsilon_I \rangle^2 + \langle \varepsilon_{II} \rangle^2 + \langle \varepsilon_{III} \rangle^2} \quad K^{-1}(z) = \alpha_t F_t(z) + \alpha_c F_c(z) \tag{20}$$

where

$$F_t(z) = 1 - \frac{\varepsilon_0(1-A_t)}{z} - \frac{A_t}{\exp\left[B_t(z-\varepsilon_0)\right]};$$

$$F_c(z) = 1 - \frac{\varepsilon_0(1-A_c)}{z} - \frac{A_c}{\exp\left[B_c(z-\varepsilon_0)\right]}.$$

α_t, α_c, ε, A_t, A_c, B_t and B_c are material constants.

The material (concrete) properties used in the simulations are the following:

G_i = initial shear modulus = 13,174.5 MPa
v_i = initial Poisson's ratio = 0.215
A_t = parameter for internal traction evolution law = 0.7858
B_t = parameter for traction damage evolution law = 8857.39
A_c = parameter for compression damage evolution law = 1.0267
B_c = parameter for compression damage evolution law = 230.71
ε_{d0} = initial damage threshold strain = 0.0001129

5.2. *Square plate subjected to vertical displacements*

The first example discussed herein is a typical square plate subjected to vertical displacements at the right side, while the left side is considered fixed. The upper and lower sides are considered as traction free. An internal grid of twenty-five subregions (cells) having the same size, were considered in order to calculate the equivalent strain at the four internal points defined at each subregion, i.e. the equivalent strain was calculated at 100 internal points in the plate. Of course, the user can define as many internal points as desired in order to refine the results. Each internal subregion is defined with four boundary linear elements (2-noded elements) thus yielding a total of 60 boundary elements and 36 nodal points. Figure 7 shows the geometry and the boundary conditions imposed to the problem, as well as the position of the internal points.

The vertical displacement imposed at the right side is $d = -0.015$ cm, which is stepwise modified with increments of 10% of the displacement value until the final value is reached.

As it is well known, this kind of problem produces a diagonal traction-stress-band from the left-upper corner to the right-lower corner of the domain, which causes the degradation of the material under consideration. Thus, the main values of the damage index are expected at these corners. Figure 8 illustrates the distribution of the damage values at an increment of 70% of the prescribed displacement and Fig. 9 shows the map of equivalent strains.

Note that the damage distribution is located around the described diagonal traction-band, as expected. Figure 10 displays the damage values obtained when the total value (100%) of the vertical displacement is applied to the plate. Values of the damage index up to 0.7 are obtained before the failure of the plate.

This simple example shows that the proposed approach is able to detect the critical zones of the domain, based on a simple and efficient scalar non-local damage model, as discussed previously.

Several numbers of internal points were also used in order to see how this number can affect the results. The analysis of the numerical results showed that the damage values were essentially the same when using a larger number of internal points (9 and 16 internal points at each cell).

Also, sensitivity analyses were carried out to assess the robustness of the procedure and its

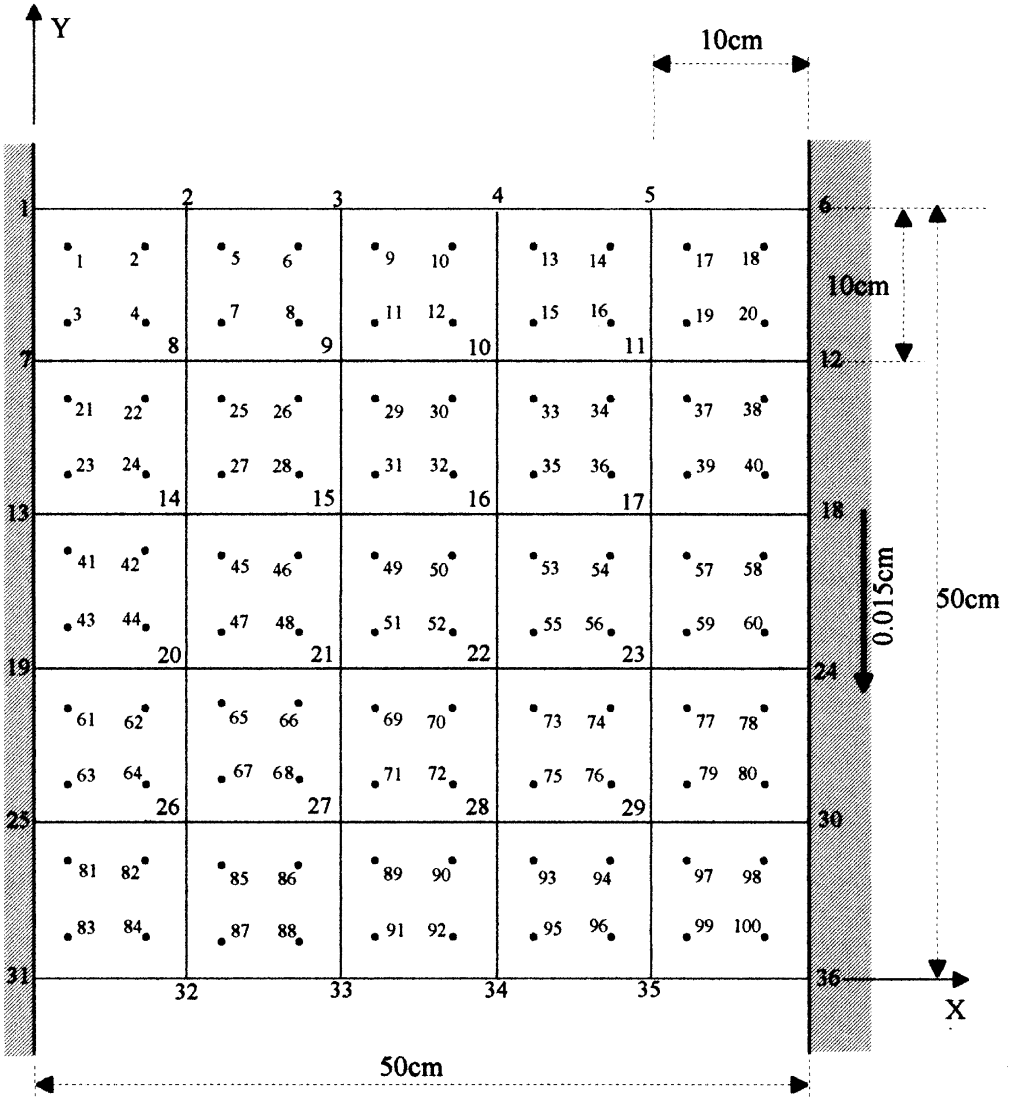

Fig. 7. Square plate subjected to vertical displacements: geometry, boundary conditions and internal points (4 boundary elements for subregion).

independence on the number of boundary elements used to discretize the domain. The same example is now discretized by using two more refined boundary-element meshes. These new meshes were defined with the same number of subregions (25 internal cells), but now each one of them was defined with both eight and twelve linear boundary elements. Also, four internal points by cell were used in these meshes, as displayed in Fig. 11.

Figures 12 and 13 show the damage distribution for the δ-element-cell mesh at 70% and 100% of the imposed displacement. Note that the results are quite similar to those obtained when using

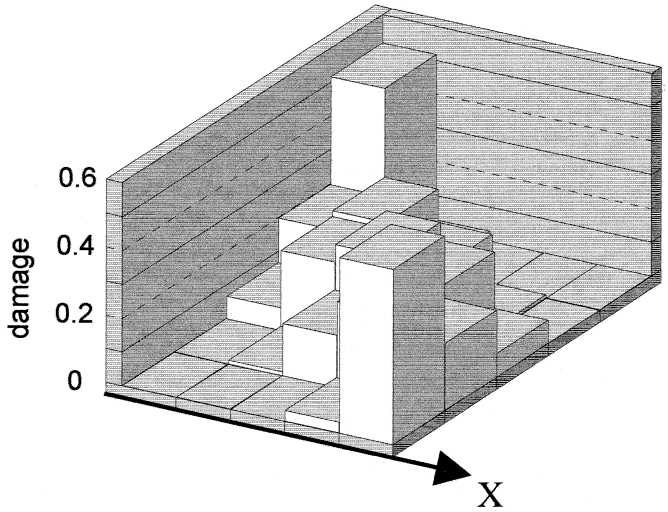

Fig. 8. Damage distribution in square plate (4 boundary elements for subregion): 70% of the total displacement.

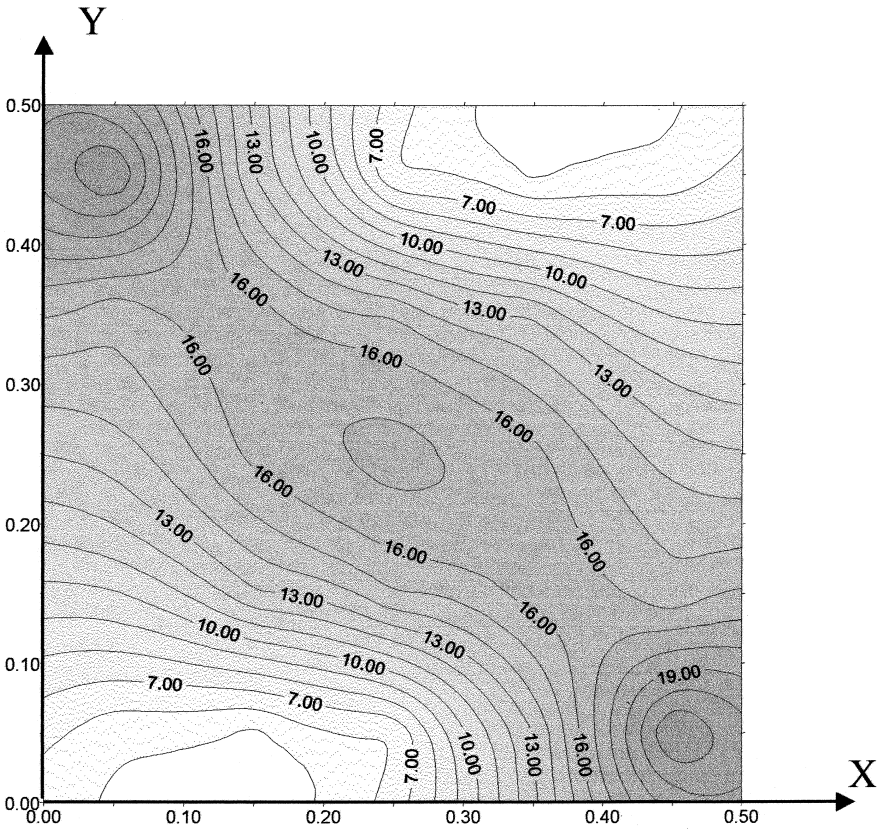

Fig. 9. Equivalent strains in square plate: 70% of the total imposed displacements (values are multiplied by 1.0 E5).

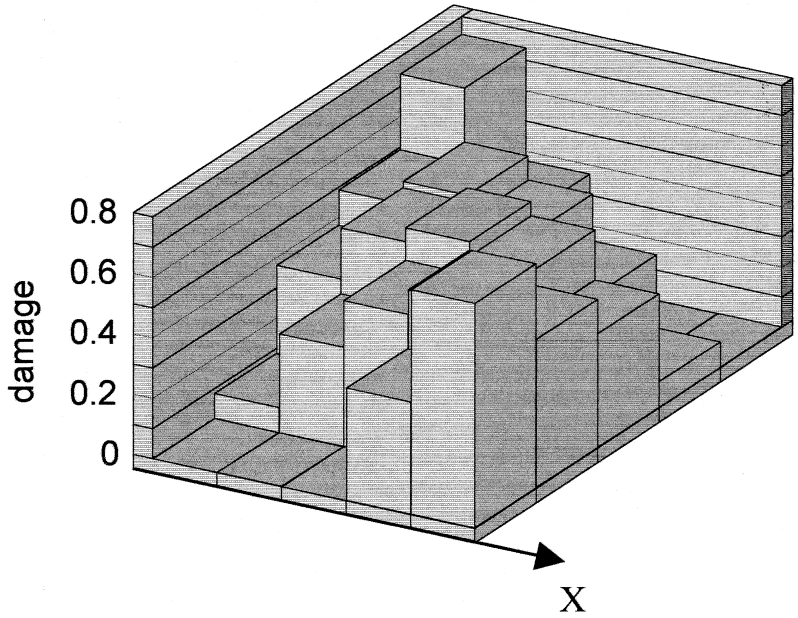

Fig. 10. Damage distribution in square plate (4 boundary elements for subregion): 100% of the total displacement.

a more simple mesh, thus confirming that the numerical algorithm is stable and independent of the degree of refinement of the boundary element mesh.

5.3. *L-shaped plate*

This example studies the behavior of an L-shaped plate which is subjected to horizontal displacements on its left side, while the right side of the plate is assumed to be fixed. Now, sixteen internal subregions (cells) are used to discretize the domain, while it was necessary to define 32 linear boundary elements and 21 nodal points, as shown in Fig. 14.

In this example, nine internal points were used in the subregions close to the singular point (internal corner), since it is expected that the highest values of the damage will be obtained at these cells. Four internal points were used in the rest of the cells. Figure 15 displays the damage distribution at 60% of the total imposed displacement, showing a clear concentration of high damage values in zones close to the singular point. Figure 16 shows the map of equivalent strains.

Figure 17 displays the damage distribution in the L-shaped plate but now at 100% of the imposed displacement. Note that damage values close to 0.8 are obtained before the failure of the plate.

It should be remarked here that sensitivity analyses were carried out to assess the result independence with respect to the boundary discretization. The damage values obtained are in good agreement with those obtained with the mesh shown in Fig. 14. The differences are of less than 5%.

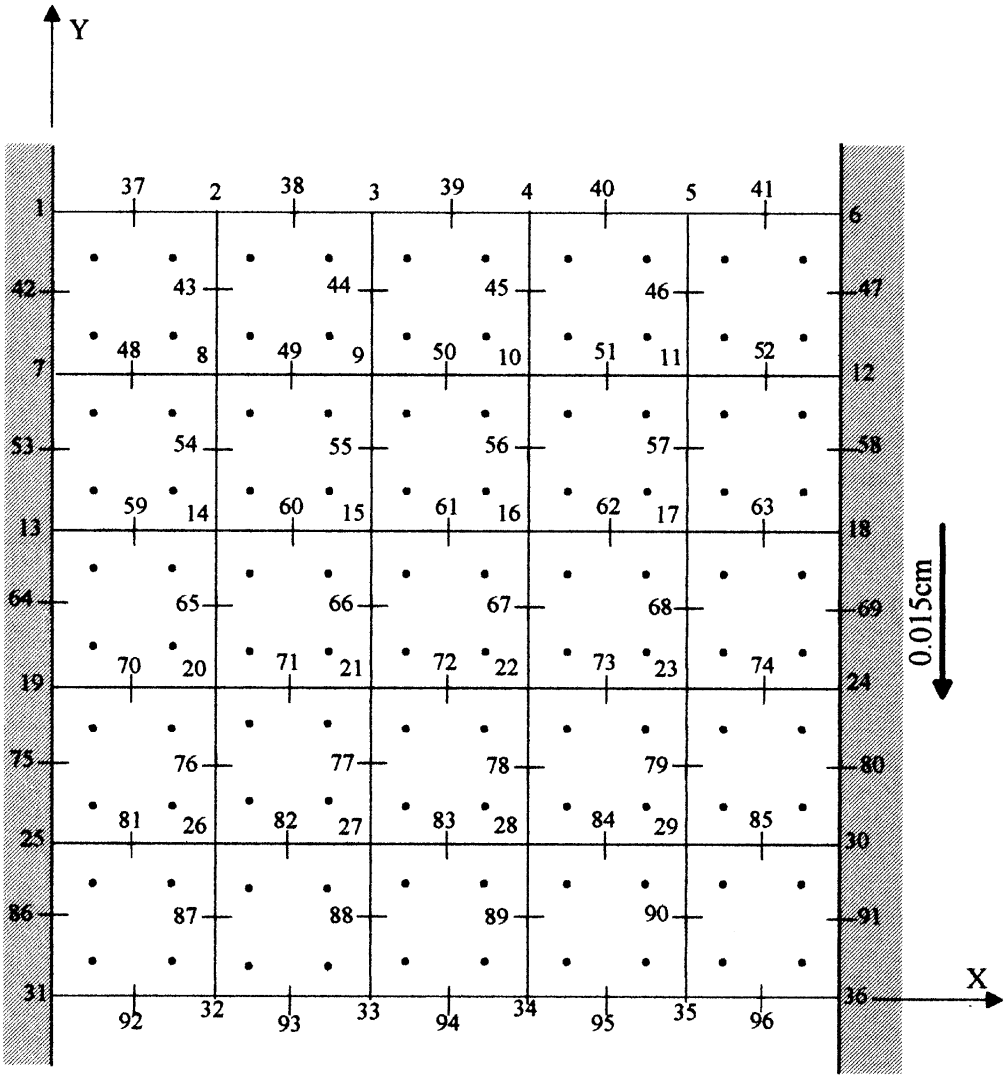

Fig. 11. Square plate: geometry, boundary conditions and internal points (8 boundary elements for subregion).

6. Concluding remarks

It has been shown in the literature, and illustrated in this paper with two simple examples, that the use of continuum damage mechanics requires the use of some regularization procedure. The implementation of these procedures in standard structural analysis programs is therefore a priority if damage models are to be used in industrial applications. Nonlocal and grid models are among the most important regularization schemes but their implementation in FE codes requires extensive modifications of the programs and the storage of a significantly larger amount of data with respect to local models.

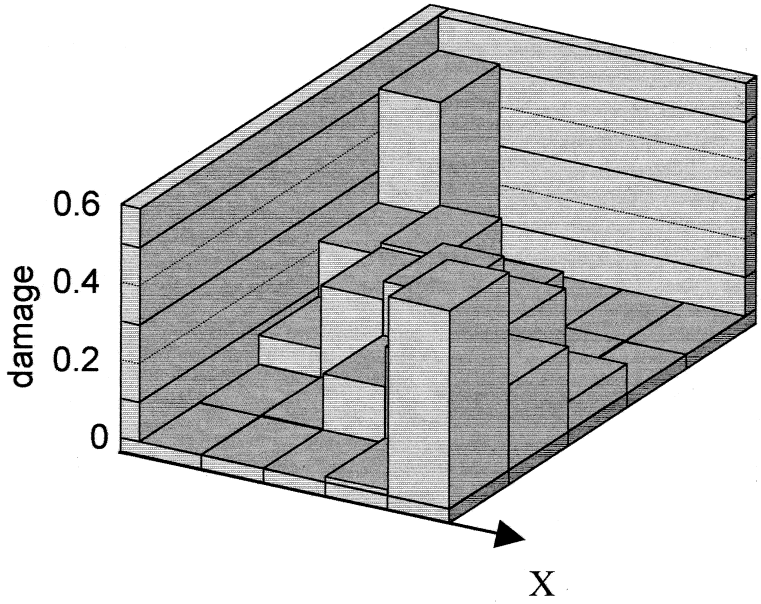

Fig. 12. Damage distribution in square plate (8 boundary elements for subregion): 70% of the total displacement.

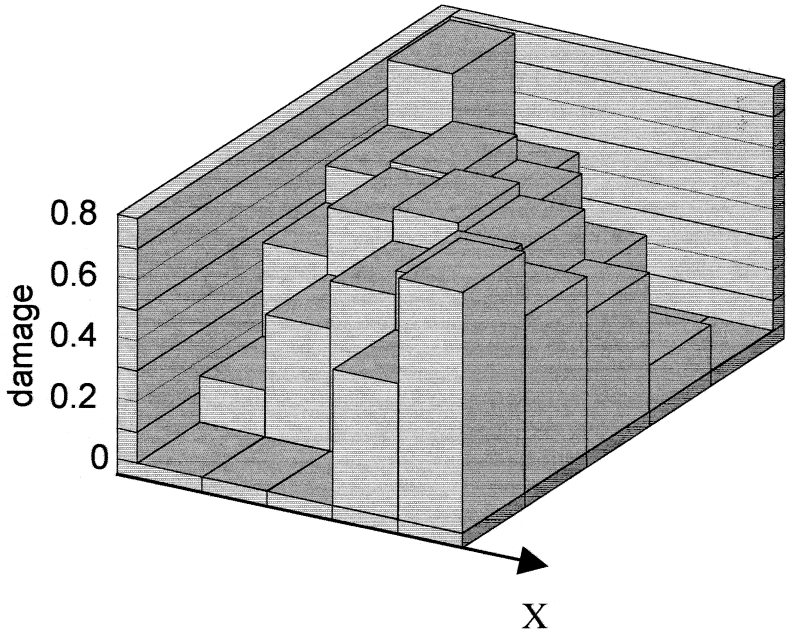

Fig. 13. Damage distribution in square plate (8 boundary elements for subregion): 100% of the total displacement.

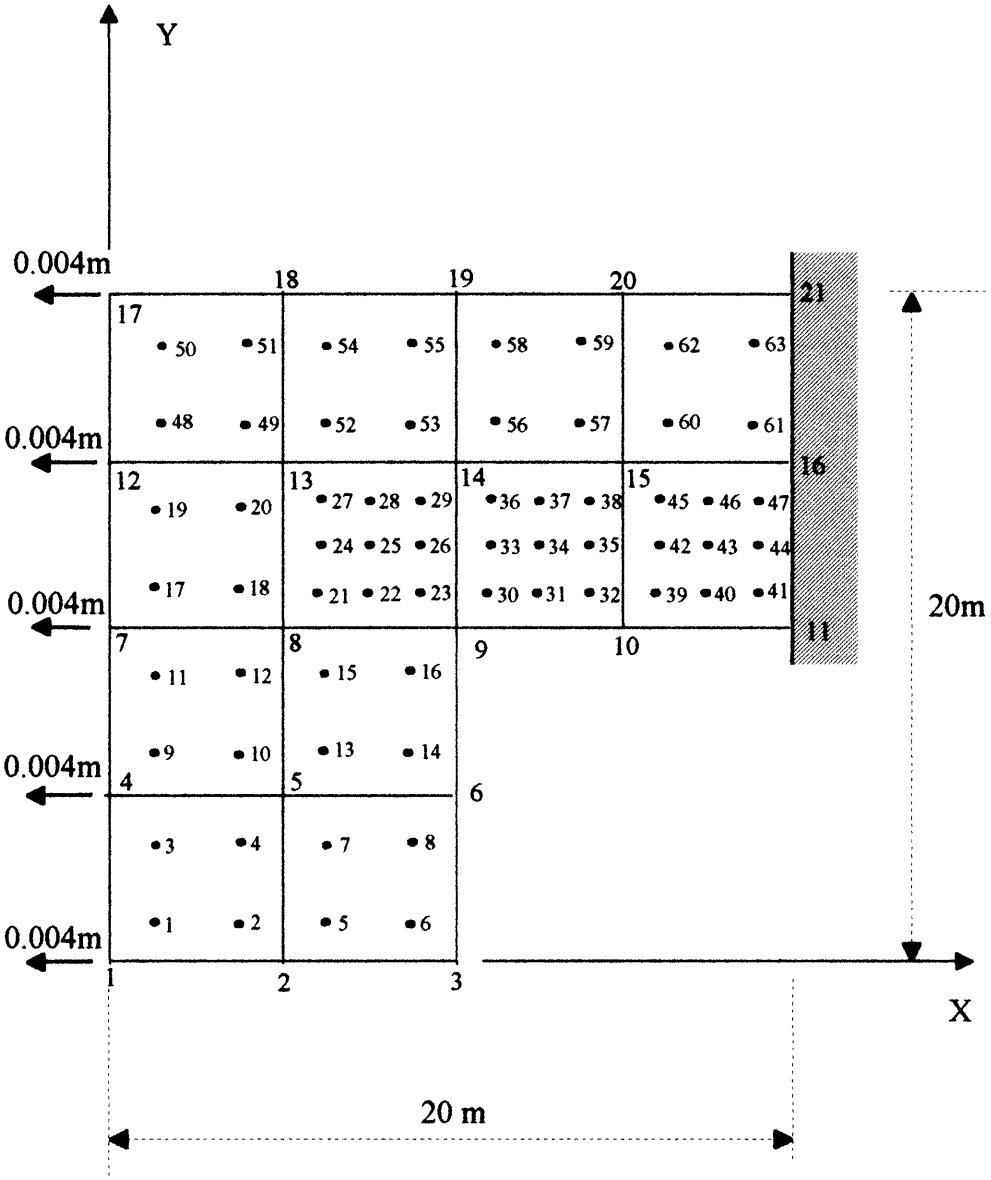

Fig. 14. L-shaped plate subjected to horizontal displacements: geometry, boundary conditions and internal points.

On the other hand, it has been shown in this paper that any standard BE program can be adapted to damage analysis of structures using grid models with very little computational effort. Very simple preprocessors can prepare the grid from the geometry of the structure. Refinements of the solution can be made very easily, by increasing the number of the mesh nodes on the grid, and the number of integration points in the cells. In summary: for the particular cases considered in this paper, it is clear that the BEM shows notable advantages over any other numerical method.

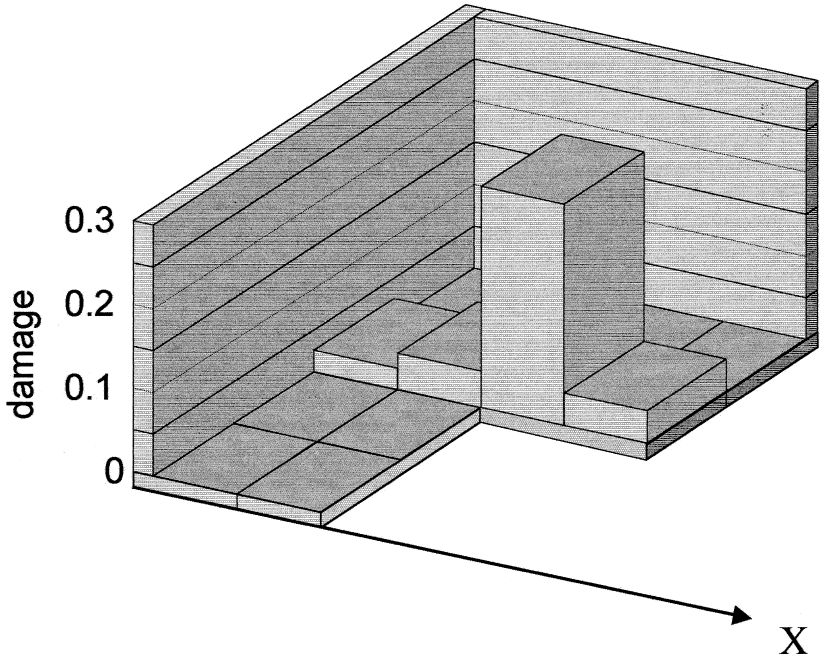

Fig. 15. Damage distribution in L-shaped plate: 60% of the total displacement.

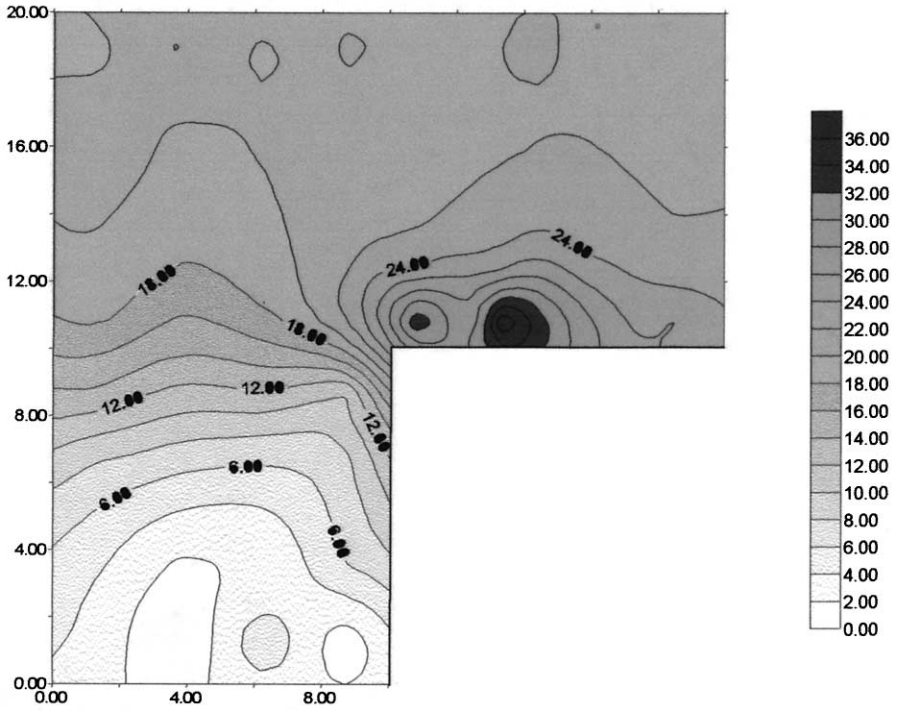

Fig. 16. Equivalent strains in L-shaped plate: 60% of the total imposed displacements (values are multiplied by 1.0 E5).

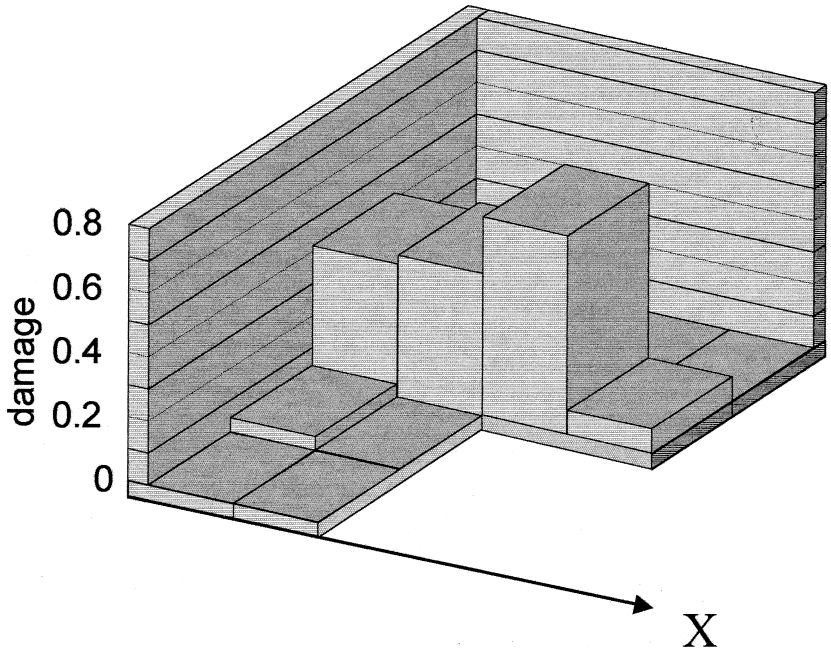

Fig. 17. Damage distribution in L-shaped plate: 100% of the total displacement.

Only two-dimensional examples were presented in this paper but it is evident that the development of a program for the three-dimensional case could also be obtained from the existent codes without difficulty. It is the opinion of the authors that in the general three-dimensional case, the advantages of the BE formulation proposed in this paper over the FE methods currently used would be significantly amplified.

However, it is clear that the framework considered in this work is restricted (grid-damage and time-independent models without plasticity) and that the extension to more general cases are still to be done. Therefore, the remarks of the two previous paragraphs are valid for the very particular cases analyzed in this paper.

Acknowledgements

The authors wish to express their acknowledgement to the C.D.C.H. of the Central University of Venezuela (Caracas), the C.D.C.H.T. of the University of Los Andes (Mérida) and CONICIT of Venezuela for their support to this research.

References

Abeyaratne, R., Knowles, J., 1990. On the driving traction acting on a surface of strain discontinuity in a continuum. J. Mech. Phys. Solids 38, 345–360.

Belytschko, T., Lasry, D., 1988. Localization limiters and numerical strategies for strain-softening materials. In: Mazars, J., Bazant, Z.P. (Eds.), Strain Localization and Size effect due to cracking and damage France-U.S. workshop.

Benallal, A., Doghri, I., Billardon, R., 1988. An integration algorithm and the corresponding consistent tangent operator for fully coupled elastoplastic and damage equations. Communications in Applied Numerical Methods 4, 731–740.

Billardon, R., Flórez-López, J., 1991. On a damage-softening model with progressive localization. In: Proc. II Pan American Congress of Applied Mechanics. Valparaiso, Chile.

Brebbia, C.A., Telles, J.C., Wrobel, L., 1984. Boundary element techniques: theory and applications in engineering, Springer Verlag, Berlin.

Brekelmans, W.A.M., Schreurs, P.J.G., De Vree, J.H.P., 1992. Continuum damage mechanics for softening of brittle materials. Acta Mech. 93, 133–143.

Cerrolaza, M., Alarcón, E., 1989. A bicubic transformation for the numerical evaluation of Cauchy Principal Value integrals. Int. J. of Num. Meth. in Eng. 28(1), 987–999.

Cerrolaza, M., García, R., 1997. Boundary elements and damage mechanics to analyze excavations in rock mass. J. of Eng. Anal. with Bound. Elem. 20, 1–16.

Cervera, M., Oliver, J., Faria, R., 1995. Seismic evaluation of concrete dams via continuum damage models, Earthquake Eng. and Struct. Dyn. 24, 1225–1245.

Chen, Z., Ailor, M., Gray, L. J., 1990. Interior point evaluation in the boundary element method, Eng. Analysis with Bound. Elem. 13, 201–208.

Crouch, S.L., Starfield, A.M., 1993. Boundary element methods in solid mechanics, George Allen & Unwin Ltd. (Publish.), London.

De Borst, R., 1990. Simulation of localization using Cosserat Theory. In: N. Bicanic, H. Mang (Eds.), Conf. on Computer Aided Analysis and Design of Concrete Structures. Pineridge Press Pub., 931–944.

De Vree, J.H.P., Brekelmans, W.A.M., Van Gils, M.A.J., 1995. Comparison of nonlocal approaches in continuum damage mechanics. Comp. & Struc. 55, 581–588.

Flórez-López, J., 1998. Continuum damage mechanics and frame analysis. Eur. J. Mech. 17, 3.

Flórez-López, J., Benallal, A., Geymonat, G., Billardon, R., 1994. A two-field finite element formulation for elasticity coupled to damage. Computer Methods in Applied Mechanics and Engineering 114, 3–4.

Gray, L.J., 1993. Symbolic computation of hypersingular boundary in integrals. In: Kane, Maier, Tosaka, Atluri (Eds.), Advances in Boundary Element Techniques. Springer Verlag, Berlin.

Hall, F.R., Hayhurst, D.R., 1991. Modelling of grain size effects in creep crack growth using a nonlocal continuum damage approach. Proc. R. Soc. Lond. A 433, 405–421.

Hult, J., 1974. Creep in continua and structures. In Leman, J.L., Ziegler, F. (Eds.), Topics in Applied Continuum Mechanics, Springer, Berlin, pp. 137–155.

Kachanov, L.M., 1958. On creep rupture time. IZV. AKAD. NAUK. SSSR 8, 26–31.

Kane, J., 1994. Boundary element analysis in engineering continuum mechanics. Prentice Hall, Englewood Cliffs, New Jersey.

Krajcinovic, D., Sumarac, D., 1989. A mesomechanical model of brittle deformation process. J. Appl. Mech. 56, 51–62.

Leckie, F.A., Hayhurst., H., 1974. Creep rupture of structures. Proc. R. Soc. London, Ser. A 240, 323–347.

Lemaitre, J., 1992. A Course on Damage Mechanics. Springer-Verlag, Berlin.

Lemaitre, J., Chaboche, J.-L., 1978. Aspect phénoménologique de la rupture par endommagement. J. Mécanique Appliquée 2, 3.

Liqing, Liu, Katsabanis, P.D., 1997. Development of a continuum damage model for blasting analysis. Int. J. Rock. Mech. Min. Sci. 34, 217–231.

Lubliner, J., Oliver, J., Oller, S., Oñate, E., 1989. A plastic-damage model for concrete. Int. J. Solids Structures 25, 299–326.

Ma, F., Kuang, Z.B., 1995. Continuum damage mechanics treatment of constraint in ductile fracture. Engng Fracture Mech. 51, 615–628.

Marigo, J.J., 1982. Etude numérique de l'endommagement. Bull. D.E.R. Electricité de France 2, 27–48.

Mazars, J., 1986. A model of unilateral elastic damageable material and its application to concrete. In: Whittmann, F.H. (Ed.), Proc. of Fracture Toughness and Fracture Energy of Concrete. Elsevier, 61–71.

Murakami, S., 1983. Notion of continuum damage mechanics and its application to anisotropic creep damage theory. J. Engng Mat. 105, 99–105.

Pijaudier-Cabot, G., Bazant, Z.P., 1987. Nonlocal damage theory. J. Engng Mech. 113, 1512–1533.

Rabotnov, I.N., 1963. On the equations of state for creep. In: Progress in Applied Mechanics—the Prager Anniversary Volume, pp. 307–315.

Saudiris, C., Mazars, J., 1988. A multiscale approach to distributed damage and its usefulness for capturing structural size effects. In: Mazars, J., Bazant, Z.P. (Eds.), Strain Localization and Size effect due to cracking and damage France-U.S. workshop, pp. 391–403.

Sellers, E., Sheele, F., 1996. Prediction of anisotropic damage in experiments simulating minig in witwatersrand quartzite blocks. Int. J. Rock. Mech. Min. Sci. 33, 659–670.

Suaris, W., 1987. A damage theory for concrete incorporating crack growth characteristics. In: Desai et al. (Eds.), Constitutive laws for engineering materials. Elsevier, pp. 931–938.